JOURNAL OF SOLID STATE CHEMISTRY 136, 193–198 (1998)
ARTICLE NO. SC977675

Decomposition of Spinel-Type Nickel Chromium Indium Sulfides—X-Ray Powder Structure Determination

H. D. Lutz, Ch. Kringe, K. Mohn, and Th. Stingl

Anorganische Chemie I, Universität Siegen, D-57068 Siegen, Germany

Received May 5, 1997; in revised form September 26, 1997; accepted October 23, 1997

DEDICATED TO PROFESSOR HARTMUT BÄRNIGHAUSEN ON THE OCCASION OF HIS 65TH BIRTHDAY

The phase diagram of the quaternary system $NiCr_2S_4$–$NiIn_2S_4$–Cr_2S_3–In_2S_3 has been studied at 873 and 1223 K by X-ray powder structure determination of quenched samples. At high temperatures, spinel-type $Ni_y(Cr_{2-2x}In_{2x})_{1-y}S_{3-2y}$ solid solutions are formed in a large range of composition (y: 0–0.5, x: 0.3–1). At temperatures below 1183 K, these solid solutions decompose to Cr-rich and In-rich spinel-type sulfides, whereby nickel is enriched in the Cr-rich compounds. The decomposition of the spinel-type sulfides is greatly retarded, even at temperatures about 900 K, due to both thermodynamic and kinetic reasons. The cation distribution established corresponds to a site preference as $Cr^{3+} > Ni^{2+} > In^{3+}$ at the octahedral 16d site and □ (vacancies) $> In^{3+} > Ni^{2+}$ at the tetrahedral 8a site of the spinel structure. The metal-sulfur distances of the solid solutions refined are compared with those calculated from characteristic metal–sulfur distances in close-packed structures, taking into account the site occupation established. For the respective indium-sulfur distances, the following improved values are recommended: $In_{tet}–S = 247.1$ pm; $In_{oct}–S = 260.6$ pm. © 1998 Academic Press

Key Words: **nickel chromium indium sulfides; spinel-type; X-ray powder structure determination; cation distribution; mechanism of decomposition; characteristic indium(III)–sulfur distances**

INTRODUCTION

Normal spinel-type chromium sulfides MCr_2S_4 and partially inverse spinel-type indium sulfides MIn_2S_4 (M = Mn, Fe, Co, and Ni) display complete mutual solid solubility at elevated temperatures (1–6). These solid solutions show spin glass behavior at low temperatures. They decompose at temperatures below 1050–1300 K (depending on M) to chromium-rich and indium-rich spinel-type solid solutions (5–8). The sections with constant M^{II} content deviate more or less from quasibinary behavior. Thus, for M = Co, the bivalent metal is enriched in the chromium rich solid solution (8). Therefore, the true composition of the phases formed on decomposition cannot be deduced from the unit-cell dimensions alone (8). In the case of M = Ni, in addition to a chromium-rich and an indium-rich spinel-type solid solution, in some cases formation of a third spinel-type sulfide has been observed (7, 9). The rates of the decomposition reactions under investigation, which have been assumed to be spinodal (6, 8), however, are extremely small (6, 7).

In this work, we have studied nickel chromium indium sulfides before and after decomposition using X-ray powder structure determination techniques in order to establish (i) composition and cation distribution of the various spinel-type compounds formed; (ii) the site preference of the metal ions involved; (iii) the phase diagram of the system under study; and (iv) the mechanism of decomposition of the spinel-type solid solutions. In addition, the metal–sulfur distances refined should be compared with those calculated from the characteristic metal–sulfur distances in close-packed structures proposed by Kesler (10).

EXPERIMENTAL

Monophase nickel chromium indium sulfide spinel-type solid solutions were prepared by heating appropriate mixtures of the binary sulfides NiS, Cr_2S_3, and In_2S_3 in evacuated, closed silica tubes at 1223 K for three days. For details see Ref. (7, 9, 11). Decomposition to Cr-rich and In-rich solid solutions was established by annealing the monophase samples for three months at 873 K (11).

The samples obtained were characterized by X-ray Guinier powder photographs (Huber 600 system) using Cu$K\alpha_1$ radiation and α-quartz as an internal standard. The unit-cell dimensions of the spinel-type solid solutions were computed from the respective spinel-structure patterns by least squares methods (LSUCR (12)).

The X-ray powder diffraction intensities were measured with an MZ IV and a PTS 1000 Seifert powder diffractometer using Cu$K\alpha$ radiation. The measuring ranges (2ϑ) used for structure refinement were 10–80° and the step width was 0.02°. For diffractometer control, data collection, and transfer into ASCII format, the program package XDAL 3000 (13) was used. The background was determined

0022-4596/98 $25.00

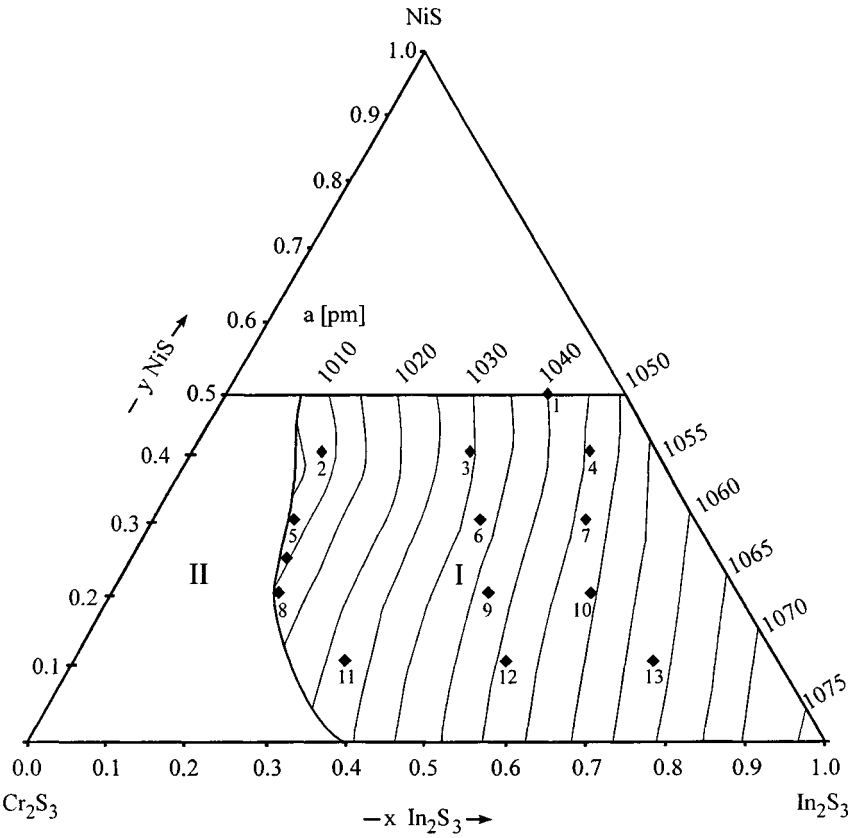

FIG. 1. The phase diagram of the quaternary system $NiCr_2S_4$–$NiIn_2S_4$–Cr_2S_3–In_2S_3 at 1223 K with respect to the formula $Ni_y(Cr_{2-2x}In_{2x})_{1-y}S_{3-2y}$ as established in (7,11); I: spinel-type solid solutions; II: multi-phase (spinel-type and deficient NiAs superstructure-type compounds); contour lines: samples with equally large unit-cell dimensions; ◆: samples characterized by X-ray powder structure determinations; and figures: samples as in Tables 1–6).

graphically. The structures were refined with the Rietveld program FullProf (14). In order to avoid correlation between the various parameters, refinement was performed in the order: scaling factor, zero shift, unit-cell dimension, halfwidth parameter W, mixing parameter of the Pseudo-Voigt function η, asymmetry parameter, then the fractional coordinates x, y, and z (u), the overall thermal parameter $B_{overall}$, the profile parameters U and V, and the occupation factors. In the final refinement, all parameters were varied with the exception of $B_{overall}$. Convergence is reached when the standard deviations of all parameters differ less than 11% for the last two cycles. Furthermore, the Cr^{3+} ions were located solely at the octahedral sites because of their high octahedral site preference and the vacancies were located only at the tetrahedral sites (15). The concentration of the vacancies was derived from the molar fraction of Ni^{2+} and then fixed. Further details of data collection and structure refinement are given in Ref. (11).

RESULTS

The composition of the samples studied are marked in the phase diagram given in Fig. 1. Samples with equal unit-cell dimensions are connected by contour lines (7,11). A Rietveld refinement plot of a decomposed $Ni_{0.14}Cr_{1.57}In_{1.0}S_4$ sample is shown in Fig. 2. The crystal data and the experimental parameters of structure refinement are given in Tables 1 and 2[1], the fractional atomic coordinates and the occupation factors in Tables 3–5, and interatomic distances in Table 6. The phase diagram of the system $NiCr_2S_4$–$NiIn_2S_4$–Cr_2S_3–In_2S_3 at 873 K due to the formula $Ni_y(Cr_{2-2x}In_{2x})_{1-y}S_{3-2y}$ is shown in Fig. 3. The margins of error of the composition of the coexisting spinel-type solid solutions are $\Delta x = 0.02$–0.03 and $\Delta y = 0.04$–0.08. They are estimated from the errors of the occupation factors. In the case of some chromium-rich samples, e.g. 2 and 3, the decomposition partly resulted in not fully equilibrated phases (see Fig. 3). In the case of the samples 6, 9, and 10, three different spinel-type solid solutions were formed with the decomposition experiment (see Fig. 3).

[1]Additional material to this paper can be ordered by referring to CSD 407126–407147, the names of the authors, and citations of the paper at the Fachinformationszentrum Karlsruhe, Gesellschaft für wissenschaftlich-technische Information mbH, D-76344 Eggenstein-Leopoldshafen, Germany. The lists of the F_o/F_c data are available from the authors up to one year after the publication has appeared.

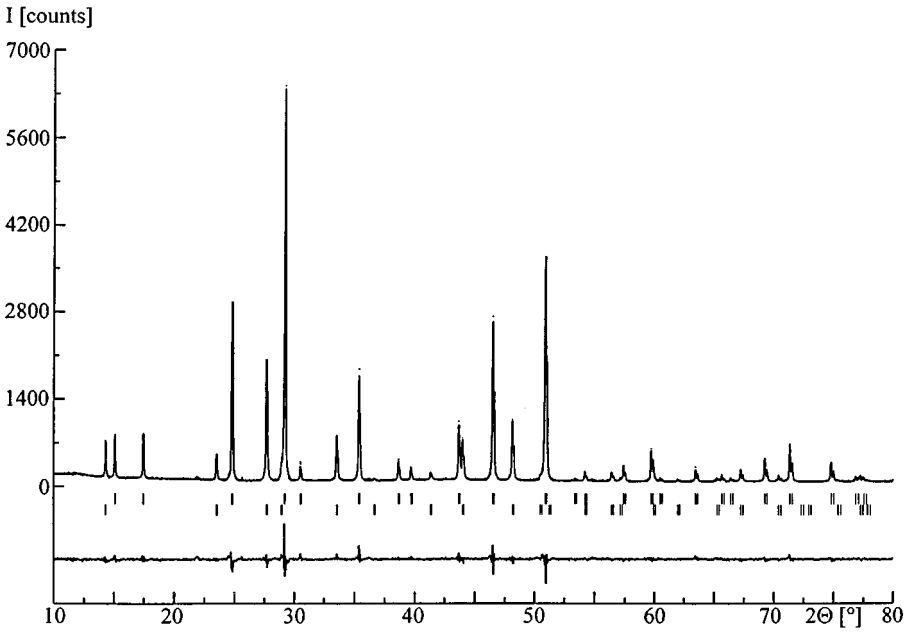

FIG. 2. Observed (·····), fitted (—), and difference X-ray diffraction profiles of $Ni_{0.14}Cr_{1.57}In_{1.0}S_4$ decomposed at 873 K. Calculated 2Θ values of the two spinel-type solid solutions are marked with vertical bars (|).

Cation Distribution and Metal–Sulfur Distances of Spinel-type Nickel Chromium Indium Sulfides

The results obtained confirm the not fully inverse cation distribution of $NiIn_2S_4$ (15) and the normal one in the case of spinel-type chromium sulfides (16). Hence, the octahedral site preference of the metal ions under investigation range as $Cr^{3+} > Ni^{2+} > In^{3+}$. The vacancies formed in the case of nickel-deficient compounds are located solely on the

TABLE 1

Crystal Data and Experimental Parameters of the Structure Determination of Monophase Spinel-type Nickel Chromium Indium Sulfides (Sample Nos. as Shown in Fig. 1, Refinement in Space Groups *Fd$\bar{3}$m* and *F$\bar{4}$3m* for Samples 5, 8, and 11, respectively)[a]

No.	Composition	*a* (pm)[b]	R_{Bragg} (%)	GoF[c]
1	$NiCr_{0.4}In_{1.6}S_4$	1039.41(2)	8.95	1.04
2	$Ni_{0.73}Cr_{1.56}In_{0.62}S_4$	1007.40(1)	3.28	1.6
3	$Ni_{0.73}Cr_{0.87}In_{1.31}S_4$	1029.20(2)	7.49	1.07
4	$Ni_{0.73}Cr_{0.36}In_{1.82}S_4$	1046.35(2)	5.46	0.929
6	$Ni_{0.5}Cr_{0.93}In_{1.40}S_4$	1032.64(2)	6.18	0.860
7	$Ni_{0.5}Cr_{0.5}In_{1.83}S_4$	1046.56(2)	6.74	1.75
9	$Ni_{0.31}Cr_{0.90}In_{1.56}S_4$	1035.46(3)	6.72	0.944
10	$Ni_{0.31}Cr_{0.62}In_{1.85}S_4$	1048.12(2)	5.86	1.17
12	$Ni_{0.14}Cr_{1.0}In_{1.57}S_4$	1040.52(2)	6.28	1.06
13	$Ni_{0.14}Cr_{0.50}In_{2.07}S_4$	1057.42(2)	5.21	0.994
5	$Ni_{0.5}Cr_{1.75}In_{0.56}S_4$	1005.09(1)	5.82	1.74
8	$Ni_{0.31}Cr_{1.85}In_{0.62}S_4$	1009.72(2)	6.71	1.62
11	$Ni_{0.14}Cr_{1.57}In_{1.0}S_4$	1022.03(2)	4.22	1.34

[a] No. of observations: 3248–3501; No. of reflections: 15–18, No of parameters: 11–13.

[b] Data obtained from X-ray Guinier powder photographs are given in Ref. (11).

[c] Goodness of fit.

TABLE 2

Crystal Data and Experimental Parameters of the Structure Determination of Multiphase Spinel-type Nickel Chromium Indium Sulfides after Decomposition at 873 K (Refinement in Space Group *Fd$\bar{3}$m*, Composition of the Starting Materials for Samples 2–13 as Given in Table 1)[a]

No.	2	3	4	11	13
a (pm)[b]	1001.00(2)	1005.61(3)	1043.05(1)	1013.73(1)	1009.48(3)
	1019.25(2)	1032.20(3)	1066.70(3)	1068.03(2)	1065.99(2)
R_{Bragg} (%)	4.94	9.75	7.54	3.72	7.51
	4.92	5.31	8.73	6.70	5.03
GoF[c]	1.02	0.745	0.97	1.19	0.96
No.	6	9	10[d]	10[e]	
a (pm)[b]	1007.87(3)	1009.86(3)	1007.66(3)	1007.05(3)	
	1035.27(3)	1035.10(4)	1035.03(3)	1034.71(3)	
	1062.3(1)	1061.9(1)	1063.0(1)	1063.6(1)	
R_{Bragg} (%)	6.98	4.13	7.34	8.52	
	6.43	5.56	7.78	6.93	
	6.61	4.05	6.38	6.82	
GoF[c]	1.02	0.889	1.03	1.32	

[a] No. of observations: 3248–3501; No. of reflections: 28–32; No. of parameters: 21–33.

[b] Data obtained from X-ray Guinier powder photographs are given in Ref. (11).

[c] Goodness of fit.

[d] For decomposition, the sample was annealed for two months at 873 K.

[e] For decomposition, the sample was annealed for four months at 873 K.

TABLE 3
Fractional Atomic Coordinates and Occupation Factors of Monophase Spinel-type Nickel Chromium Indium Sulfides Refined in Space Group $Fd\bar{3}m$

No.	Composition[a]	Fractional coordinate[b]	Occupation factors[c] 8a site In	8a site Ni	16e site Cr	16e site Ni	16e site In
1	$NiCr_{0.4}In_{1.6}S_4$	0.2632(2)	0.94	0.06	0.37(1)	0.94	0.69(1)
2	$Ni_{0.73}Cr_{1.56}In_{0.62}S_4$	0.2620(2)	0.72(5)	0.19(5)	1.47(5)	0.54(5)	–
3	$Ni_{0.73}Cr_{0.87}In_{1.31}S_4$	0.2636(3)	0.91	—	0.84(2)	0.73	0.43(2)
4	$Ni_{0.73}Cr_{0.36}In_{1.82}S_4$	0.2602(2)	0.91	—	0.35(1)	0.73	0.92(1)
6	$Ni_{0.5}Cr_{0.93}In_{1.40}S_4$	0.2624(2)	0.83	—	0.89(1)	0.50	0.61(1)
7	$Ni_{0.5}Cr_{0.5}In_{1.83}S_4$	0.2606(3)	0.83	—	0.52(1)	0.50	0.98(1)
9	$Ni_{0.31}Cr_{0.99}In_{1.48}S_4$	0.2617(2)	0.77	—	0.90(1)	0.31	0.79(1)
10	$Ni_{0.31}Cr_{0.62}In_{1.85}S_4$	0.2584(2)	0.78	—	0.63(1)	0.31	1.06(1)
12	$Ni_{0.14}Cr_{1.0}In_{1.57}S_4$	0.2607(2)	0.71	—	0.97(1)	0.14	0.89(1)
13	$Ni_{0.14}Cr_{0.50}In_{2.07}S_4$	0.2587(3)	0.71	—	0.54(5)	0.14	1.32(5)

[a] As synthesized, that calculated from the occupation factors agrees within the standard deviations given.
[b] Fractional atomic co-ordinate ($u = x = y = z$) of S (32e site), those of the tetrahedral 8a and octahedral 16e sites are 1/8 and 1/2, respectively.
[c] With respect to the formula $M_{tet}M_{oct2}S_4$, data without standard deviations have not been refined.

tetrahedral 8a site of the spinel structure. In the case of Cr-rich samples with nearly equal amounts of Ni^{2+} and vacancies and In^{3+} at the tetrahedral sites, superstructure ordering of the tetrahedrally coordinated metal ions due to space group $F\bar{4}3m$ is observed (see Table 4). In this case, the tetrahedral 4c site with M–S distances of 242–249 pm is fully occupied by In^{3+} ions. The remainder of the In^{3+} ions, the Ni^{2+} ions, and the vacancies are placed at the smaller 4a site with M–S distances of 227–234 pm (see Tables 4 and 6).

Phase Diagram of the System $NiCr_2S_4$–$NiIn_2S_4$–Cr_2S_3–In_2S_3 at 873 K

The compositions of the spinel-type nickel chromium indium sulfides obtained after decomposition at 873 K (see Table 5) reveal non-quasibinary behavior of the system as shown in Fig. 3. That is, the nickel ions are enriched in the Cr-rich spinel-type solid solutions as already evidenced for the respective cobalt compounds (8). The cation distribution of the spinel-type phases formed on decomposition agrees with that of the monophase samples of the same composition, so far as can be determined with sufficient accuracy.

DISCUSSION

Non-quasibinary Behavior of the Spinel-type Sulfides

The enrichment of the Ni^{2+} ions in the chromium-rich spinel-type solid solutions and, hence, the non-quasibinary behavior is obviously the result of one or more of the following aspects: (i) the relatively low octahedral site preference of Ni^{2+} ions, at least as compared to that of Cr^{3+}; (ii) the nearly equal characteristic Ni–S and Cr–S distances compared to the larger one of In–S (10); (iii) the preference of Ni^{2+} ions for more covalent sulfides rather than more ionic ones as in the respective indium compounds, and (iv) the gain of additional cohesive energy on forming (quaternary) spinel-type nickel chromium sulfides with much smaller unit cells than those of the respective indium sulfides.

Characteristic In(III)–S Distances

The metal-sulfur distances at the various sites determined by the structure refinement deviate significantly from those calculated from characteristic M–S distances (10) with

TABLE 4
Fractional Atomic Coordinates and Occupation Factors of Monophase Spinel-type Nickel Chromium Indium Sulfides Refined in Space Group $\bar{F}43m$

No.		5	8	11
Composition[a]		$Ni_{0.5}Cr_{1.75}In_{0.56}S_4$	$Ni_{0.31}Cr_{1.85}In_{0.62}S_4$	$Ni_{0.14}Cr_{1.57}In_{1.0}S_4$
Fractional coordinates[b]	16e: M_{oct}	0.6307(3)	0.6309(3)	0.6300(2)
	16e: S(1)	0.3919(3)	0.3904(4)	0.3880(3)
	16e: S(2)	0.8693(4)	0.8679(5)	0.8679(3)
Occupation factors[c]	4a: In(1)	0.186(5)	0.131(5)	0.200(1)
	Ni(1)	0.144(5)	0.150(5)	—
	16e: Cr	1.686(5)	1.840(5)	1.558(1)
	Ni(2)	0.313(5)	0.161(5)	0.143
	In(3)	—	—	0.300(1)

[a] As synthesized, that calculated from the occupation factors agrees within the standard deviations given.
[b] Fractional atomic coordinate ($x = y = z$) of In(1) and Ni(1) (4a) = 0, that of In(2) (4c) = 1/4.
[c] Occupation factors (with respect to the formula $M_{tet}(1)_{0.5}M_{tet}(2)_{0.5}M_{oct2}S(1)_2S(2)_2$), that of In(2) (4c) is 0.5, those of S(1) and S(2) are 2.0, data without standard deviations are not refined.

TABLE 5

Fractional Atomic Coordinates and Occupation Factors of Multiphase Spinel-type Nickel Chromium Indium Sulfides (Space Groups $Fd\bar{3}m$ and $F\bar{4}3m$) after Decomposition at 873 K (Composition of the Starting Materials for Samples 2–13 as given in Table 1)

			Fractional coordinates[b]		
No.	Composition[a]	Mol%	16e (M_{oct})	16e (S)	32e (S)
2	$Ni_{0.73}Cr_{1.61}In_{0.57}S_4$	62.1	0.6302(2)	0.3906(3), 0.8708(4)	—
	$Ni_{0.73}Cr_{1.25}In_{0.93}S_4$	37.9	—	—	0.2634(2)
3	$NiCr_{1.52}In_{0.48}S_4$	18.5	—	—	0.2637(5)
	$Ni_{0.73}Cr_{0.77}In_{1.41}S_4$	81.5	—	—	0.2620(2)
4	$Ni_{0.73}Cr_{0.54}In_{1.64}S_4$	88.4	—	—	0.2613(2)
	$Ni_{0.24}Cr_{0.01}In_{1.75}S_4$	11.6	—	—	0.257(1)
11	$Ni_{0.14}Cr_{1.75}In_{0.82}S_4$	82.1	0.6293(3)	0.3882(3), 0.8650(3)	—
	$Ni_{0.14}Cr_{0.07}In_{2.51}S_4$	17.9	—	—	0.2574(5)
13	$Ni_{0.50}Cr_{1.77}In_{0.56}S_4$	14.7	0.6343(9)	0.393(1), 0.875(2)	—
	$Ni_{0.11}Cr_{0.31}In_{2.29}S_4$	85.3	—	—	0.2573(2)
6	$Ni_{0.61}Cr_{1.66}In_{0.60}S_4$	24.8	0.630(1)	0.387(1), 0.869(2)	—
	$Ni_{0.61}Cr_{0.82}In_{1.45}S_4$	52.0			0.2601(3)
	$Ni_{0.14}Cr_{0.38}In_{2.20}S_4$	23.3			0.2575(7)
9	$Ni_{0.50}Cr_{1.70}In_{1.38}S_4$	33.0	0.6291(7)	0.3882(8), 0.868(1)	—
	$Ni_{0.40}Cr_{1.02}In_{1.38}S_4$	22.0			0.2588(6)
	$Ni_{0.14}Cr_{0.36}In_{2.22}S_4$	45.0			0.2563(3)
10[d]	$Ni_{0.49}Cr_{1.77}In_{0.56}S_4$	14.0	0.6348(7)	0.392(1), 0.877(2)	—
	$Ni_{0.50}Cr_{0.89}In_{1.54}S_4$	22.7			0.2593(5)
	$Ni_{0.22}Cr_{0.24}In_{2.28}S_4$	63.3			0.2545(2)
10[e]	$Ni_{0.49}Cr_{1.75}In_{0.58}S_4$	14.7	0.6349(8)	0.392(1), 0.880(2)	—
	$Ni_{0.50}Cr_{0.94}In_{1.40}S_4$	19.2			0.2599(6)
	$Ni_{0.22}Cr_{0.27}In_{2.25}S_4$	66.1			0.2536(2)

	Occupation factors[c]				
	Tetrahedral sites: 4a ($F\bar{4}3m$), 8a ($Fd\bar{3}m$)		Octahedral sites: 16e, 16d		
No.	In	Ni	Cr	Ni	In
2	0.073(4)	0.337(4)	1.607(4)	0.392(4)	—
	0.93(1)	—	1.25(1)	0.73	—
3	0.48(2)	0.52(2)	1.52(2)	0.48(2)	—
	0.91	—	0.77(1)	0.73	0.50(1)
4	0.91	—	0.54(1)	0.73(1)	0.73
	0.77	—	0.01	0.24(7)	1.75(7)
11	0.21	—	1.75(1)	0.14	0.11(1)
	0.71	—	0.07(3)	0.14	1.80(3)
13	0.06(2)	0.27(2)	1.77(2)	0.23(2)	—
	0.71	—	0.31(1)	0.11	1.58(1)
6	0.10(1)	0.27(1)	1.66(1)	0.34(1)	—
	0.88	—	0.82(2)	0.61	0.57(2)
	0.71	—	0.38(4)	0.14	1.49(4)
9	0.13(1)	0.20(1)	1.70(1)	0.30(1)	—
	0.80	—	1.02(3)	0.40	0.58(3)
	0.72	—	0.36(2)	0.14	1.50(2)
10[d]	0.06(1)	0.26(1)	1.77(1)	0.23(1)	—
	0.84	—	0.89(3)	0.50	0.61(3)
	0.74	—	0.24(1)	0.22	1.54(1)
10[e]	0.08(5)	0.24(5)	1.75(3)	0.25(3)	—
	0.84	—	0.94(3)	0.50	0.56(3)
	0.74	—	0.27(1)	0.22	1.51(1)

[a] As calculated from the occupation factors refined.

[b] Fractional atomic coordinates ($u = x = y = z$) of the 32e site (space group $Fd\bar{3}m$) and the three (M, S(1), and S(2)) 16e sites (space group $F\bar{4}3m$); those of the 8a and 16d sites ($Fd\bar{3}m$) and the 4a and 4c sites ($F\bar{4}3m$) are 1/8 and 1/2, and 0 and 1/4, respectively.

[c] Occupation factors with respect to the formula $M_{tet}(1)_{0.5}\,M_{tet}(2)_{0.5}M_{oct2}S(1)_2S(2)_2$ and $M_{tet}M_{oct2}S_4$; those of 4c (In(2)), 16e (S(1) and S(2)), and 32e (S) are 0.5, 2, and 4, respectively. Data without standard deviations have not been refined.

[d] For decomposition, the sample was annealed at 873 K for two months.

[e] Same as for [d], but for four months.

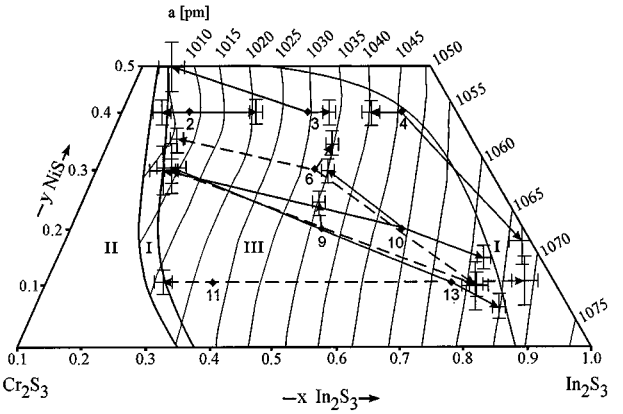

FIG. 3. Pathways of decomposition of spinel-type nickel chromium indium sulfide solid solution at 873 K; I: monophase spinel-type solid solutions; II: multiphase (see Fig. 1); III: multiphase (Cr^{3+}-rich and In^{3+}-rich spinel-type solid solutions); points of the arrows: compositions of the Cr^{3+}-rich and the In^{3+}-rich solid solutions formed (see Table 5); |—|: margins of error; for further explanations see Fig. 1.

regard to the occupation factors established (see Table 6). This is obviously caused by the too small characteristic tetrahedral In(III)–S distance proposed in (10). The calculated metal-sulfur distances can be improved by choosing a greater characteristic tetrahedral In(III)–S distance. This is obtained from the structure data of indium sulfide spinels assuming that the degree of inversion is smaller than 1, which, in fact, has been established by recent single-crystal structure refinements (15). We therefore propose 247.1 (α) and 260.6 pm (β) instead of 245.0 and 264.0 pm (10) for the characteristic In(III)–S distances of tetrahedral and octahedral units in eutactic (close-packed) sulfide structures.

Mechanisms of Decomposition of Spinel-type Chromium Indium Sulfides

The formation of three spinel-type sulfide solid solutions by decomposition experiments (see Fig. 3) led to the speculation that there is a third area of stable nickel chromium indium sulfide solid solutions in the phase diagram under investigation, *viz.* at about $x = 0.5$ (9). This, however, is not true. The reason for the occurrence of a third phase is rather the extremely low rate of the decomposition reaction. The metastable but nevertheless long-range existence of solid solutions with intermediate chromium indium content (see Table 5) and, hence, the extreme lowering of the reaction rate is caused by the competition of several kinetic and thermodynamic factors. Thus, at the beginning of decomposition, the composition of the parent compound is changed because of both the different diffusion coefficients of the metal ions involved, *e.g.*, that of Cr^{3+} is much smaller than that of In^{3+}, and the different gradients of electrochemical potential inside the crystallites (17).

TABLE 6
Metal–Sulfur Distances (pm) of Monophase Spinel-Type Nickel Chromium Indium Sulfides Refined in Space Groups $Fd\bar{3}m$ and $F\bar{4}3m$

No.	Composition[b]	MS_4 tetrahedron[c]		MS_6 octahedron[c]	
1	$(In_{0.94}Ni_{0.06})_{tet}[Cr_{0.37}Ni_{0.94}In_{0.69}]_{oct}S_4$	249.1(4)	245.6	247.3(3)	247.1
2	$(In_{0.72}Ni_{0.19}\square_{0.09})_{tet}[Cr_{1.47}Ni_{0.54}]_{oct}S_4$	239.3(3)	240.3	240.5(2)	240.7
3	$(In_{0.91}\square_{0.09})_{tet}[Cr_{0.84}Ni_{0.73}In_{0.43}]_{oct}S_4$	247.3(5)	244.9	244.2(3)	244.7
4	$(In_{0.91}\square_{0.09})_{tet}[Cr_{0.35}Ni_{0.73}In_{0.92}]_{oct}S_4$	245.6(4)	244.9	250.9(2)	249.5
6	$(In_{0.83}\square_{0.17})_{tet}[Cr_{0.89}Ni_{0.50}In_{0.61}]_{oct}S_4$	246.0(4)	243.0	246.2(2)	246.7
7	$(In_{0.83}\square_{0.17})_{tet}[Cr_{0.53}Ni_{0.50}In_{0.97}]_{oct}S_4$	245.6(4)	243.0	251.4(3)	250.3
9	$(In_{0.77}\square_{0.23})_{tet}[Cr_{0.90}Ni_{0.31}In_{0.79}]_{oct}S_4$	245.4(4)	241.6	247.5(2)	248.6
10	$(In_{0.78}\square_{0.22})_{tet}[Cr_{0.63}Ni_{0.31}In_{1.06}]_{oct}S_4$	242.5(3)	241.8	253.7(2)	251.2
12	$(In_{0.71}\square_{0.29})_{tet}[Cr_{0.97}Ni_{0.14}In_{0.89}]_{oct}S_4$	244.8(3)	240.1	249.7(2)	249.7
13	$(In_{0.71}\square_{0.29})_{tet}[Cr_{0.54}Ni_{0.14}In_{1.32}]_{oct}S_4$	244.8(5)	240.1	255.5(3)	254.3
5	$(In_{0.14}Ni_{0.19}\square_{0.17})_{tet1}(In_{0.5})_{tet2}[Cr_{1.69}Ni_{0.31}]_{oct}S_4$	227.9(8)	231.8	242.5(5)	240.7
		247.4(6)	247.1	240.1(5)	
8	$(In_{0.13}Ni_{0.19}\square_{0.22})_{tet1}(In_{0.5})_{tet2}[Cr_{1.84}Ni_{0.16}]_{oct}S_4$	230.0(7)	229.2	245.2(5)	245.5
		246.3(6)	247.1	239.8(5)	
11	$(In_{0.2}\square_{0.3})_{tet1}(In_{0.5})_{tet2}[Cr_{1.56}In_{0.30}Ni_{0.14}]_{oct}S_4$	234.0(6)	232.6	248.9(3)	244.0
		244.5(5)	247.1	243.4(4)	

Note. Second columns: mean values calculated from characteristic M–S distances from Ref. (10)[a] with regard to the occupation factors given in Tables 3 and 4

[a] In contrast to Ref. (10), 247.1 and 260.6 pm instead of 245.0 and 264.0 pm have been used as characteristic $In(III)_{tet}$–S and $In(III)_{oct}$–S distances (see text).

[b] As established by X-ray powder structure determination (see Tables 3 and 4).

[c] In the case of refinement in space group $F\bar{4}3m$ (samples 5, 8, 11), first and second lines due to M–S(1) and M–S(2) distances, respectively.

ACKNOWLEDGMENTS

The authors thank the Deutsche Forschungsgemeinschaft and the Fonds der Chemischen Industrie for financial support.

REFERENCES

1. F. K. Lotgering and G. H. A. M. van der Steen, *J. Inorg. Nucl. Chem.* **33,** 673 (1971).
2. Y. Mimura, M. Shimada, and M. Koizumi, *Solid State Commun.* **15,** 1035 (1974).
3. L. Goldstein, L. Brossard, M. Guittard, and J. L. Dormann, *Physica B and C* **86–88,** 889 (1977).
4. E. Riedel and R. Karl, *J. Solid State Chem.* **38,** 40 (1981).
5. H. D. Lutz, W. W. Bertram, B. Oft, and H. Haeuseler, *J. Solid State Chem.* **46,** 56 (1983).
6. H. D. Lutz, M. Jung, and K. Wussow, *Mater. Res. Bull.* **21,** 161 (1986).
7. Th. Schmidt and H. D. Lutz, *J. Less-Common Met.* **161,** 7 (1990).
8. J. Himmrich, B. Müller, Ch. Schöler, Th. Stingl, and H. D. Lutz, *J. Solid State Chem.* **101,** 128 (1992).
9. Th. Stingl, Doctoral Thesis, University of Siegen (1991).
10. Ya. A. Kesler, *Izv. Akad. Nauk SSSR, Neorg. Mater.* **29,** 165 (1993), *Inorg. Mater.* **29,** 145 (1993).
11. Ch. Kringe, Doctoral Thesis, University of Siegen (1996).
12. LSUCR, Least Squares Unit Cell Refinement, Programmbibliothek für Chemie, HRZ Köln.
13. XDAL 3000, program package, Fa. Seifert, Ahrensburg.
14. J. Rodriguez-Carvajal, FULLPROF: A Program for Rietveld Refinement and Pattern Matching Analysis; Abstracts of the Satellite Meeting on Powder Diffraction of the XV Congress of the International Union of Crystallography, Toulouse, France, p. 127 (1990).
15. H. D. Lutz and M. Jung, *Z. anorg. allg. Chem.* **579,** 57 (1989).
16. H. v. Philipsborn and H. Treitinger, *in* "Landolt-Börnstein, Zahlenwerte und Funktionen aus Physik," Neue Folge, III/12b, p. 300. Springer-Verlag, Berlin, 1980.
17. H. Schmalzried, private communication.